Electronic Supplementary Material (ESI) for Nanoscale.

Supporting Information

Rationally designed self-standing V_2O_5 electrode towards high voltage non-aqueous all-solid-state symmetric (2.0 V) and asymmetric (2.8 V) supercapacitors

Meena Ghosh,[12] Vidyanand Vijayakumar,[12] Roby Soni,[12] Sreekumar Kurungot[12]*

[1]Physical and Materials Chemistry Division

CSIR-National Chemical Laboratory, Pune, Maharashtra, India-411008.

E-mail: k.sreekumar@ncl.res.in

[2]Academy of Scientific and Innovative Research, Anusandhan Bhawan, 2 Rafi Marg, 110001

New Delhi, India

Equations and calculations used for electrode preparation and their performance evaluation[1]

1. Calculation:

(A) Loading of V_2O_5 per unit cm^2 area of functionalized Toray carbon paper (fCP) was calculated from the Faraday's Law as given in **equation 1**.

$$Loading\ (\frac{mg}{cm^2}) = \frac{Current\ density\ (mA)\ \times\ deposition\ time\ (sec)\ \times\ molecular\ weight\ of\ V2O5\ (182\ g/mo}{No.\ of\ electrons\ transferred\ (n) \times 96485\ C} \quad (1)$$

(B) Calculation of specific capacitance (C_s) for the device from chrono charge-discharge method is given in **equation 2.**

$$C_s = \frac{(I\ \times\ \Delta t)}{(\Delta V\ \times\ Z)} \quad (2)$$

where, I is current density used for charging-discharging, Z can be total mass of the active material on both the electrodes (for gravimetric capacitance), or total area of both the electrodes coated with the active material (for areal capacitance), or total volume of the device (for volumetric capacitance)

For the calculation of the capacitance of the single-electrode, the above equation should be multiplied with four.

(C) Calculation of Energy density (ED) and Power density (PD) are given in **equation 3** and **4**, respectively.

$$\text{ED (W h kg}^{-1}) = \frac{Cs}{2 \times 3.6} V^2 \quad (3)$$

$$\text{PD (W kg}^{-1}) = (\text{ED}) / t \quad (4)$$

t is the discharge time calculated in hour.

(D) Calculation for the mass balancing of the two electrodes for the V/fCP-x//AC/fCP-y asymmetric device (ASC) is given in **equation 5**.

$$\frac{M_+}{M_-} = \frac{C_- \times V_-}{C_+ \times V_+} \quad (5)$$

where, M is the mass loading, C is the capacitance measured individually in three electrode set-up, V is the potential of the individual electrode.

Subscripts + and - stand for the positive and negative electrodes, respectively.

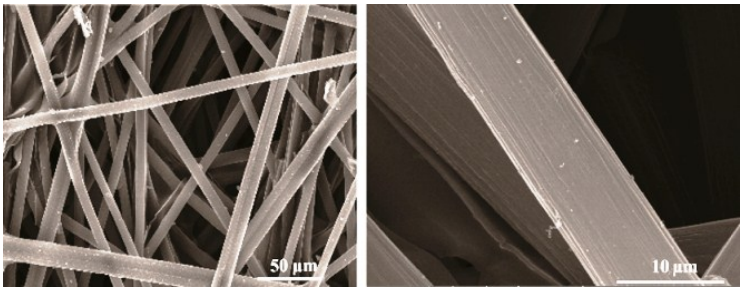

Fig. S1 FESEM images of pCP at different magnifications.

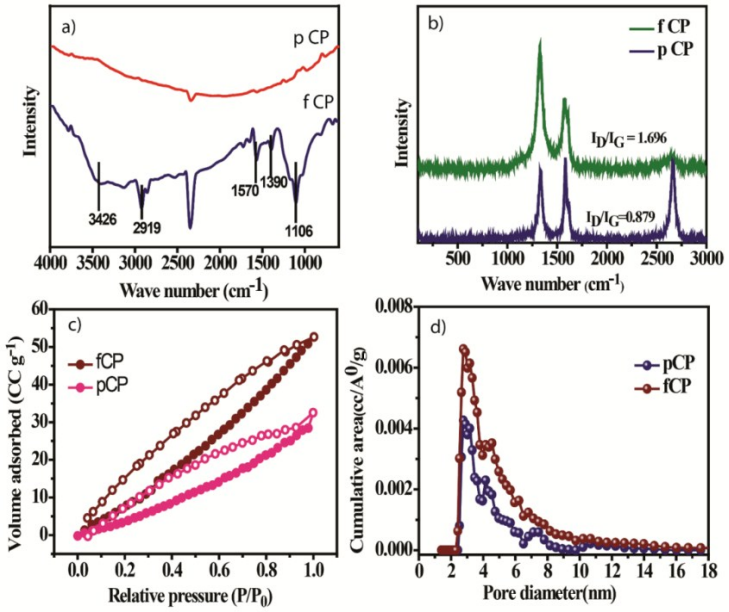

Fig. S2 Comparison of (a) IR spectra; (b) Raman spectra; (c) N_2 adsorption/desorption isotherms and (d) pore size distribution profile recorded before and after the functionalization of the carbon paper.

Presence of the functional groups on fCP is validated by FTIR spectra as given in Fig. S2a. The peaks located at 3426 and 1710 cm^{-1} in fCP correspond to the presence of oxygen functionalities (–OH stretching and C=O in –COOH, respectively). Besides, the characteristic twin peak appeared at 2919 and 2852 cm^{-1} indicate successful functionalization of the carbon paper.

In the Raman spectra, (Fig. S2b) the D band appeared at a wave number of 1339 cm^{-1} is resolved with a higher intensity after the functionalisation and I_D/I_G ratio is increased by two times. During the anodic functionalization, nucleophilic attack of OH^- induces some defect on the graphitic structure of the carbon fiber. A substantialy decreased intensity of the 2D band at 2663 cm^{-1} strongly indicates the defect rich carbon nanofibe in fCP.[2,3]

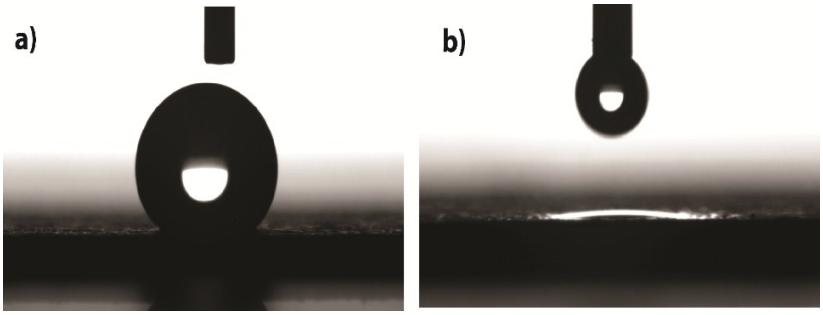

Fig. S3 Images corresponding to the contact angle measurement of (a) pCP and (b) fCP

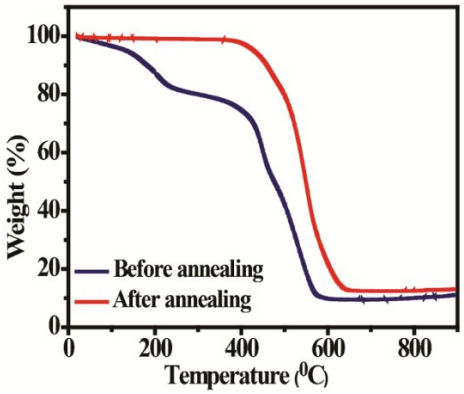

Fig. S4 TGA profiles of the V_2O_5 coated carbon paper before and after the heat treatment

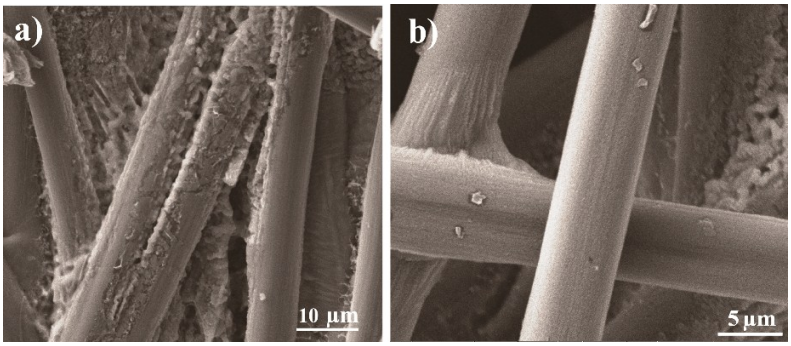

Fig. S5 SEM images of the V/pCP-177 recorded at different magnifications.

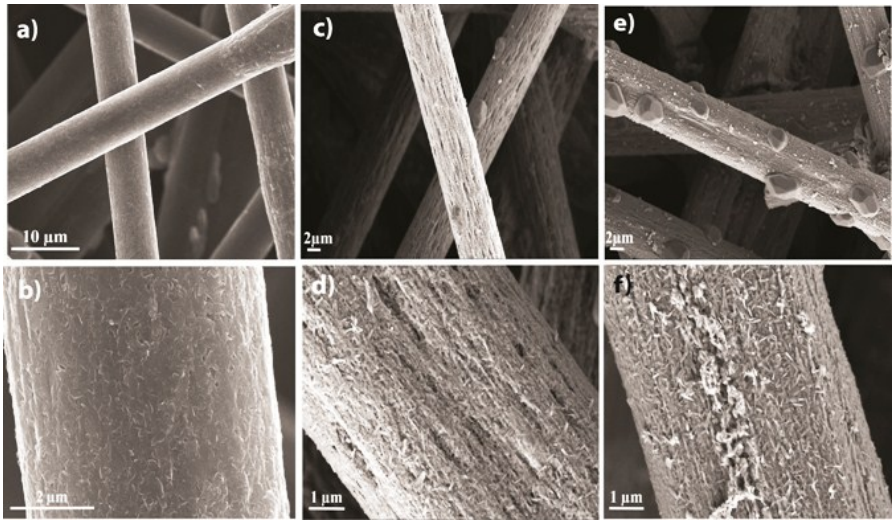

Fig. S6 FESEM images of V/fCP-88 (a and b), V/fCP-442 (c and d) and V/fCP-707 (e and f) recorded at lower and higher magnifications, respectively.

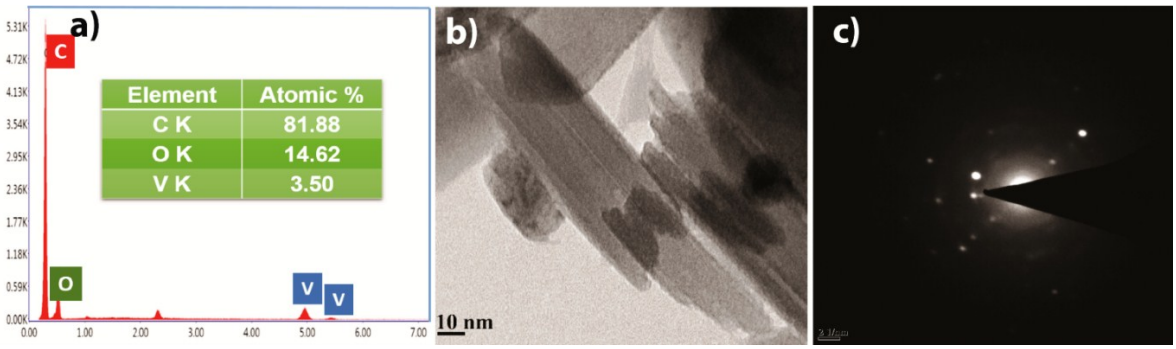

Fig. S7 (a) EDAX spectrum; (b) TEM image and (c) SAED pattern of the V_2O_5 nanoflakes corresponding to the V/fCP-177 sample.

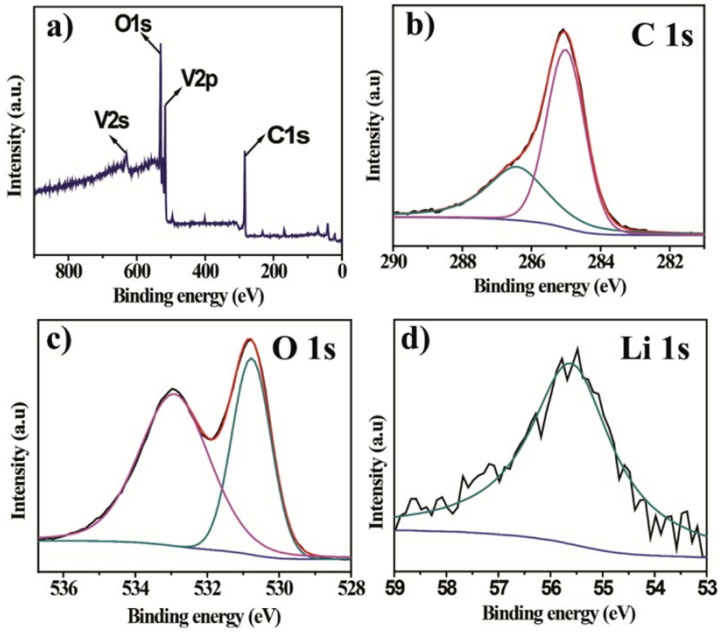

Fig. S8 (a) XPS survey spectrum of V/fCP-177 specimen; (b) deconvoluted XPS spectra of carbon (C); (c) oxygen (O) and (d) lithium (Li) in the V/fCP-177 specimen.

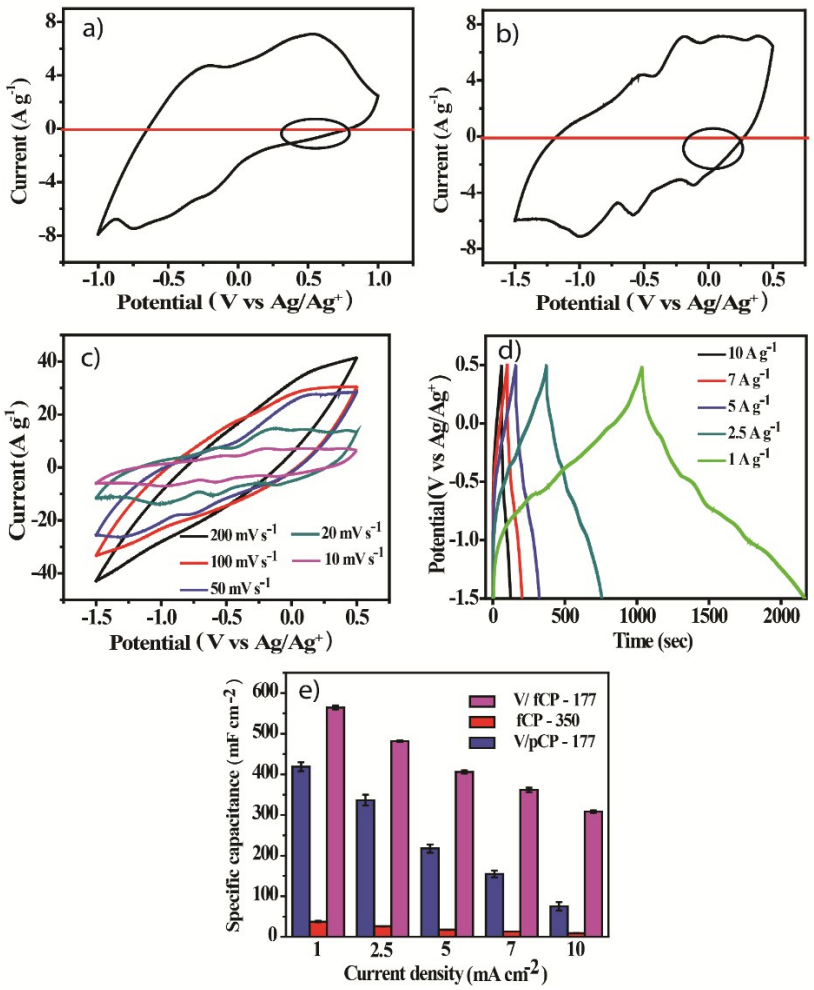

Fig. S9 (a) The CV profiles recorded at a scan rate of 10 mV s^{-1} for V/fCP-177 sample in the three-electrode configuration in the potential windows of -1.0 to +1.0 V and (b) -1.5 to +0.50 V, respectively; (c) the CV and (d) CD profiles of V/fCP-177 recorded in the potential window of -1.5 to +0.5 V; (e) error bar diagram of the specific capacitance *vs.* current density of the V/fCP-177, fCP-350 and V/pCP-177 specimens.

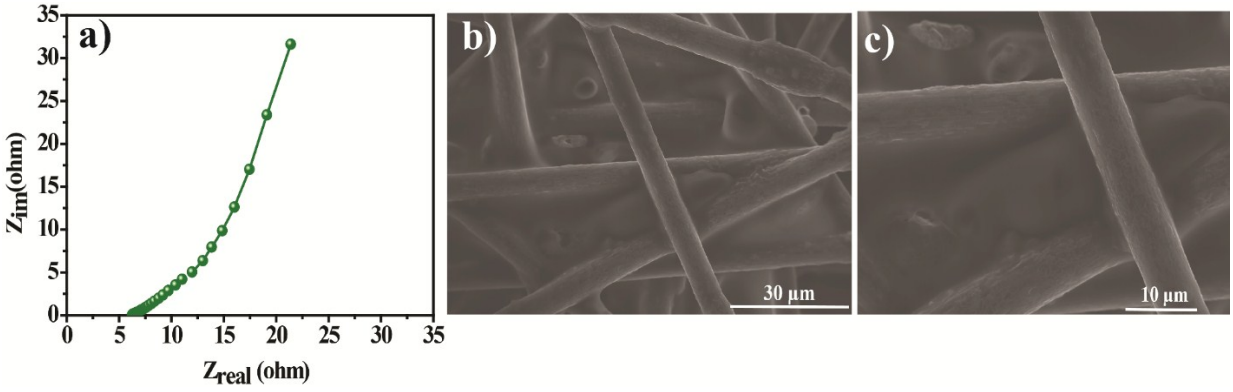

Fig. S10 (a) Nyquist plot of the V/fCP-177 based SSC; (b) and (c) are the FESEM images of the PMMA/$LiClO_4$ electrolyte coated electrode at lower and higher magnifications, respectively.

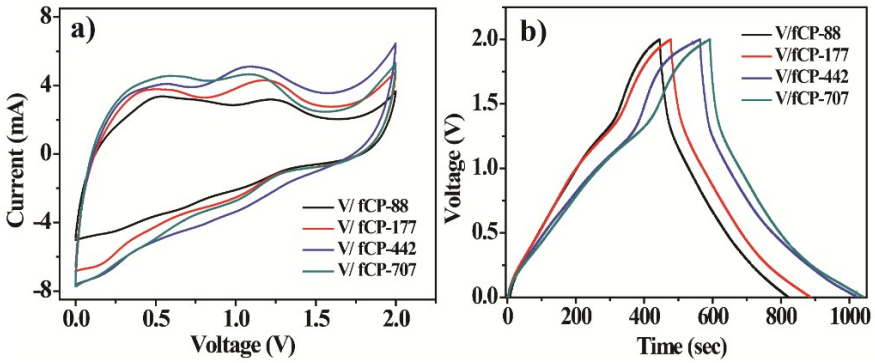

Fig. S11 Electrochemical study of the V/fCP-x based SSC (a) the CV profiles recorded at a scan rate of 20 mV s^{-1} and (b) the CD profiles recorded at a current density of 1 mA cm^{-2} measured under the same experimental conditions.

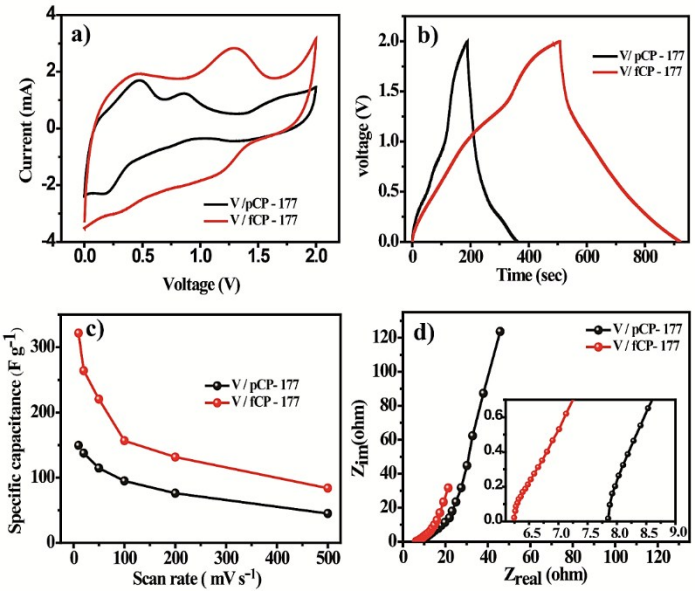

Fig. S12 (a) The CV profiles recorded at a scan rate of 10 mV s^{-1}; (b) the CD plots recorded at a current density of 1 A g^{-1} ; (c) plots representing the relationship between the specific capacitance and scan rate and (d) the Nyquist plots (inset showing the high frequency region) of the V/fCP-177 and V/pCP-177 SSC devices.

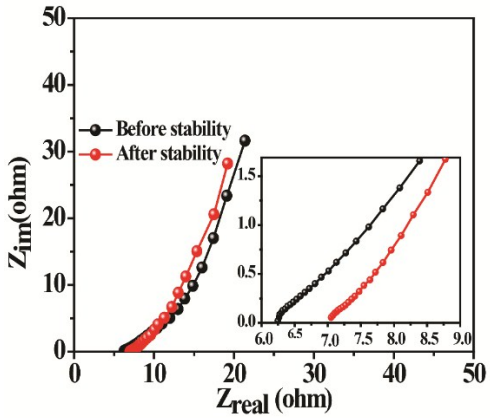

Fig. S13 Nyquist plots of the V/fCP-177 based SSC device before and after the stability test.

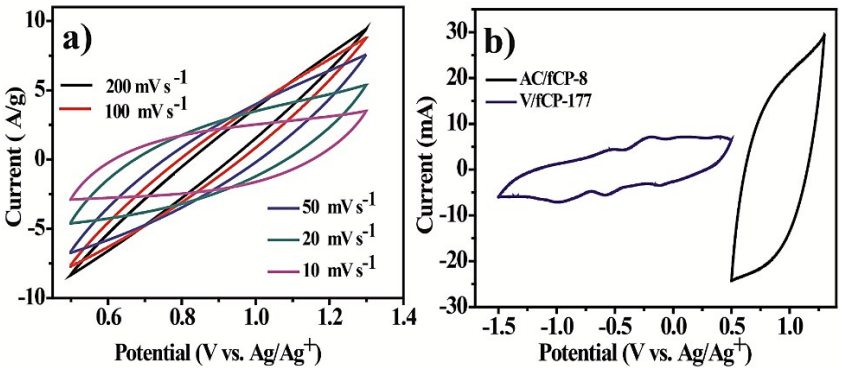

Fig. S14 (a) The CV profiles recorded at different scan rates in the case of the AC/fCP-1 electrode in the three-electrode cell assembly and (b) the CV profiles of V/fCP-177 and AC/fCP-8 recorded at a scan rate of 10 mV s^{-1} in the respective potential windows after adjusting the mass loading.

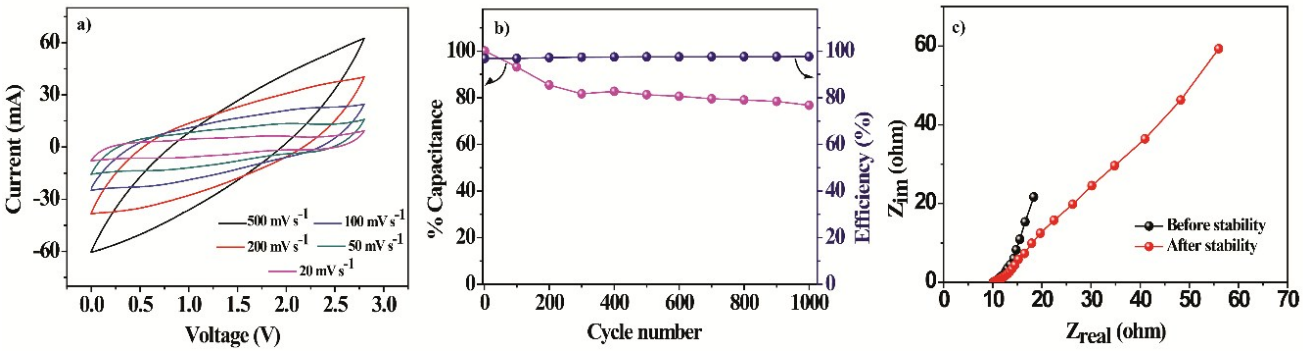

Fig. S15 (a) CV profiles recorded at different scan rates; (b) stability test and (c) Nyquist plots recorded before and after the durability test of the V/fCP-x//AC/fCP-y based ASC device.

Capacitance	**SSC device**	**ASC device**
Voltage window	2.0 V	2.8 V
Gravimetric capacitance	101.5 F g^{-1} at 0.5 A g^{-1}	94.29 F g^{-1} at 1 A g^{-1}
Volumetric capacitance	2.72 F cm^{-3}	3.176 F cm^{-3}
Areal capacitance	101.5 mF cm^{-2} at 0.5 mA cm^{-2}	117.8 mF cm^{-2} at 1 mA cm^{-2}

Table S1: Gravimetric, volumetric, areal capacitance of both SSC and ASC devices

No.	Electrode	Electrolyte	Resistance (Ω)	Capacitance	Voltage window	Reference in the main text
1	VO_2//VO_2	$LiClO_4$/PC in fumed silica	----	36 F g^{-1}	1.4 V	Ref. 33
2	V_2O_5-CNT/ITO// V_2O_5-CNT-ITO	PVA/LiCl	ESR = 29 R_{CT} ~ 7.5	74.2 F g^{-1} at 1 A g^{-1}	0.8 V	Ref. 34
3	V_2O_5/SS// V_2O_5/SS	PVA/$LiClO_4$	ESR ~ 10	52.52 F g^{-1}	1.8 V	Ref. 55
4	$LiMnO_2$// LiMnO2	PMMA/PC	----	56 F g^{-1}	1.2 V	Ref. 9
5	**V/fCP-177// V/fCP-177**	**PMMA/$LiClO_4$**	**6.3**	**101.5 F g^{-1}**	**2.0 V**	**This work**
6	V_2O_5-CNT//AC	$LiClO_4$/PC	----	42.6 F g^{-1}	2.6 V	Ref.32
7	rGO/ V_2O_5//rGO	1M $LiClO_4$/PC	3.36, R_{CT} = >30	52.5 mF cm^{-2} at 0.1 A g^{-1}	2.6 V	Ref.31
8	V_2O_5/CNT//AC	1M $NaClO_4$/PC	ESR~ 7, R_{CT} =10	35 F g^{-1}	2.8 V	Ref.56
9	V_2O_5/Gr//AC	1M $LiClO_4$/PC	----	37.2 F g^{-1} at 0.5 A g^{-1}	2.7 V	Ref.29
10	Li_3VO_4-CNF//GNS	PVDF-HFP/$LiClO_4$	R_{CT} ~ 125	45 F g^{-1} at 0.2 A g^{-1}	3.8 V	Ref.57
11	**V/fCP-44//AC/fCP-2.1**	**PMMA/$LiClO_4$**	**9.9**	**94.29 F g^{-1} at 1 A g^{-1}**	**2.8 V**	**This work**

Table S2: The cell resistance, capacitance and voltage window of both the SSC and ASC devices are compared with some of the high performance supercapacitor devices where aqueous and non-aqueous electrolytes are used with vanadium (V) and other pseudocapacitive electrode materials.

References

(1) Anothumakkool, B.; Torris A. T, A.; Bhange, S. N.; Badiger, M. V.; Kurungot, S. Electrodeposited Polyethylenedioxythiophene with Infiltrated Gel Electrolyte Interface: A Close Contest of an All-Solid-State Supercapacitor with its LiquidState Counterpart. *Nanoscale* **2014**, *6*, 5944-5952.

(2) Wang, Z.; Han, Y.; Zeng, Y.; Qie, Y.; Wang, Y.; Zheng, D.; Lu, X.; Tong, Y. Activated carbon fiber paper with exceptional capacitive performance as a robust electrode for supercapacitors *Journal of Materials Chemistry A* **2016**, *4*, 5828-5833.

(3) Zhang, H.; Qiu, W.; Zhang, Y.; Han, Y.; Yu, M.; Wang, Z.; Lu, X.; Tong, Y. Surface engineering of carbon fiber paper for efficient capacitive energy storage *Journal of Materials Chemistry A* **2016**, *4*, 18639-18645.